Direct numerical simulation of unsteady natural convection boundary layers on an evenly heated plate with time-varying heating flux

***Wenxian Lin[1,2] and S.W. Armfield[3]**

[1]School of Engineering, James Cook University,Townsville, QLD 4811, Australia.
[2]Solar Energy Research Institute, Yunnan Normal University, Kunming, Yunnan 650092, China.
[3]School of Aerospace, Mechanical and Mechatronic Engineering, University of Sydney, NSW 2006, Australia.

*Corresponding author: Wenxian.lin@jcu.edu.au

Abstract

It is of fundamental significance and application importance to fully understand the flow behavior of unsteady natural convection boundary layers under time-dependent heating conditions. Such an understanding is currently scarce. In this paper, a series of scalings developed for the major parameters representing the flow behavior of the unsteady natural convection boundary layer of a homogeneous Newtonian fluid with Pr>1 adjacent to a vertical plate evenly heated with a time-varying sinusoidal heat flux were validated by comparison to ten direct numerical simulations. These scaling provide relations between these parameters with the governing parameters of the flow, i.e., the Rayleigh number (*Ra*), the Prandtl number (*Pr*), and the dimensionless natural frequency (f_n) of the time-varying sinusoidal heat flux, at the start-up stage, at the critical time, and at the quasi-steady state. The results show that in general these scalings provide an accurate description of the flow at different development stages.

Keywords: Natural convection, boundary layer, scaling, direct numerical simulation, heat flux, time-dependent heating.

Introduction

As a classic fluid mechanics problem, owing to its fundamental and practical significance, natural convection boundary layer flow has been the subject of numerous studies. Earlier studies have focused on experimental and analytical investigations of the steady-state behavior of the flow, in particularly that on a heated semi-infinite vertical wall and in a rectangular cavity with differentially heated sidewalls (see, e.g., Hyun (1994)). More recent studies have focused on the transient flow behavior. In particular, scaling analysis has proven to be a very effective tool to reveal the transient behavior of such a flow and it has been employed to develop scalings to represent the transient behavior of natural convection boundary layers under various configurations and flow conditions (see, e.g., Patterson and Imberger (1980), Lin and Armfield (1999, 2001, 2005, 2012), Lin et al. (2007)).

Unsteady natural convection boundary layers on a vertical plate heated by a time-dependent heat flux are found in many applications, such as in the Trombe wall system of a passive solar house and in a solar chimney. In the Trombe wall case, the wall, which is usually painted in black or with a solar selective coating, absorbs solar radiation and converts it into heat which is then transported to the dwelling by the heated air via natural convection boundary layer flow in the channel formed by the glazing and the wall. A solar chimney operates in a similar manner. For both cases, the time-dependent solar radiation, which varies sinusoidally under a clear sky condition (only in the first half of the sinusoidal cycle), serves as the heat flux for the natural convection boundary-layer flows.

Although there have been numerous studies on natural convection boundary layers on a vertical plate heated by a heat flux, the majority of these studies have been on the cases where the applied heat flux is either uniformly constant or spatially varied but not time dependent (see, e.g., Armfield et al. (2007), Lin et al. (2009), Patterson et al. (2009), Bednarz et al. (2009), Saha et al. (2012), Capobianchi and Aziz (2012)). The studies on unsteady natural convection boundary layers on a vertical plate heated by a time-dependent heat flux are currently lacking, which motivates this study.

Governing equations and scalings

Under consideration is the unsteady natural convection boundary layer of a homogeneous Newtonian fluid with Pr>1 adjacent to a vertical plate evenly heated with a time-varying sinusoidal heat flux in the form of

$$\frac{dT}{dX} = -\Gamma_w(t) = -\Gamma_{wm}\sin(2\pi ft), \tag{1}$$

where T is temperature, X is the horizontal coordinate, $\Gamma_w(t)$ is the transient temperature gradient across at the plate at time instant t, Γ_{wm} is the maximum temperature gradient across at the plate, and f is the natural frequency of the time-varying flux applied to the plate. The flow is assumed to be two-dimensional and the fluid is initially at rest. The plate lies at X=0 with the origin at Y=0 (Y is the vertical coordinate), with the plate boundary conditions,

$$U = V = 0,\ \frac{dT}{dX} = -\Gamma_{wm}\sin(2\pi ft) \text{ at } x = 0 \text{ for } Y > 0,\ t \ge 0, \tag{2}$$

where Γ_{wm} and and f are assumed to be constant for a specific time-varying flux condition.

Governing equations

The governing equations of motion are the Navier-Stokes equations with the Boussinesq approximation for buoyancy, which together with the temperature equation can be written in the following dimensionless, two-dimensional forms,

$$\frac{\partial u}{\partial x} + \frac{\partial v}{\partial y} = 0, \tag{3}$$

$$\frac{\partial u}{\partial \tau} + u\frac{\partial u}{\partial x} + v\frac{\partial u}{\partial y} = -\frac{\partial p}{\partial x} + \frac{Pr}{Ra^{2/5}}\left(\frac{\partial^2 u}{\partial x^2} + \frac{\partial^2 u}{\partial y^2}\right), \tag{4}$$

$$\frac{\partial v}{\partial \tau} + u\frac{\partial v}{\partial x} + v\frac{\partial v}{\partial y} = -\frac{\partial p}{\partial y} + \frac{Pr}{Ra^{2/5}}\left(\frac{\partial^2 v}{\partial x^2} + \frac{\partial^2 v}{\partial y^2}\right) + Pr\,Ra^{1/5}\theta, \tag{5}$$

$$\frac{\partial \theta}{\partial \tau} + u\frac{\partial \theta}{\partial x} + v\frac{\partial \theta}{\partial y} = \frac{1}{Ra^{2/5}}\left(\frac{\partial^2 \theta}{\partial x^2} + \frac{\partial^2 \theta}{\partial y^2}\right), \tag{6}$$

where Ra and Pr are the Rayleigh number and the Prandtl number, defined as

$$Ra = \frac{g\beta\overline{\Gamma}_w H^4}{\nu k},\ Pr = \frac{\nu}{\kappa}, \tag{7}$$

in which g is the acceleration due to gravity which acts in the negative y-direction, β, ν and κ are the thermal expansion coefficient, kinematic viscosity and thermal diffusivity of the fluid, H is the height of the plate, and $\overline{\Gamma}_w$ is the time-averaged temperature gradient across the plate thickness calculated by

$$\overline{\Gamma}_w = \frac{1}{t_{total}}\int_0^{t_{total}} \Gamma_{wm}\sin(2\pi ft)dt = \frac{2}{\pi}\Gamma_{wm}, \tag{8}$$

where t_{total} is the total heating time of the time-varying flux applied. In this paper, it is assumed that $2\pi f t_{total}=\pi$, i.e., $f=0.5/t_{total}$ (hence only the first half heating cycle is considered, which is in line with the time-dependent solar radiation model under a clear sky condition, although the results obtained here are not limited to only the cases driven by time-dependent solar radiation). Apparently, Ra defined above is the time-averaged global Rayleigh number for the unsteady natural convection boundary layer over the duration of heating under the time-varying flux applied to the plate.

In the above governing equations, x, y, u, v, τ, p, and θ are respectively the dimensionless forms of X, Y, U, V, t, P, and T, which are the horizontal and vertical coordinates, horizontal and vertical

velocity components, time, pressure, and temperature. x, y, u, v, τ, p, and θ are made dimensionless by their respective characteristic scales as follows,

$$x=\frac{X}{H}, y=\frac{Y}{H}, u=\frac{U}{V_0}, v=\frac{V}{V_0}, \tau=\frac{t}{\left(H/V_0\right)}, p=\frac{P}{\rho V_0^2}, \theta=\frac{T-T_a}{\overline{T}_w}, \tag{9}$$

in which H is the characteristic length scale, T_a is the initial temperature of the ambient fluid, $V_0=\kappa Ra^{2/5}/H$ is the characteristic velocity scale, $\overline{T}_w=\overline{\Gamma}_w H=2\Gamma_{wm}H/\pi$ is the characteristic temperature difference scale, respectively.

Scalings

With the initiation of the flow, a vertical boundary layer will be developed adjacent to the plate, experiencing a start-up stage dominated by one-dimensional conduction, followed by a transitional stage during which a transition to two-dimensional convection occurs, before eventually attaining a quasi-steady state, with the transition time scale τ_s to separate the start-up stage and the transitional stage, as illustrated in Fig. 1, where a typical numerically simulated time series of the dimensionless thermal boundary-layer thickness δ_T at height y=0.5 for the specific case of Ra=10^8, Pr=7 and f_n=0.1 ($fn=f/(V_0/H)$ is the dimensionless natural frequency of the time-varying flux applied) is shown. Similar behavior is also observed for the other parameters to represent the transient behavior of an unsteady natural convection boundary layer on a vertical plate evenly heated with a time-varying heat flux, i.e., the plate temperature, θ_w, the maximum vertical velocity within the boundary layer, v_m, and the inner viscous boundary-layer thickness, δ_{vi}, as shown in Fig. 2.

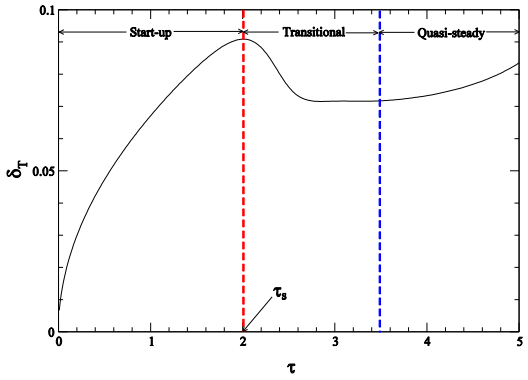

Figure 1. The three development stages of an unsteady natural convection boundary layer.

We have developed the following dimensionless scalings for the unsteady natural convection boundary layer of a homogeneous Newtonian fluid with Pr>1 adjacent to a vertical plate evenly heated with a time-varying sinusoidal heat flux:

1. *At the start-up stage:*

$$\delta_T \sim \frac{\tau^{1/2}}{Ra^{1/5}}, \tag{10}$$

$$\delta_{vi} \sim \frac{\tau^{1/2}}{\left(1+Pr^{-1/2}\right)Ra^{1/5}}, \tag{11}$$

$$\theta_w \sim \left(\frac{\pi}{2}\right)\frac{\sin\left(2\pi f_n\tau\right)\tau^{1/2}}{Ra^{1/5}}, \tag{12}$$

$$v_m \sim \left(\frac{\pi}{2}\right)\frac{\sin\left(2\pi f_n\tau\right)\tau^{3/2}}{\left(1+Pr^{-1/2}\right)^2}. \tag{13}$$

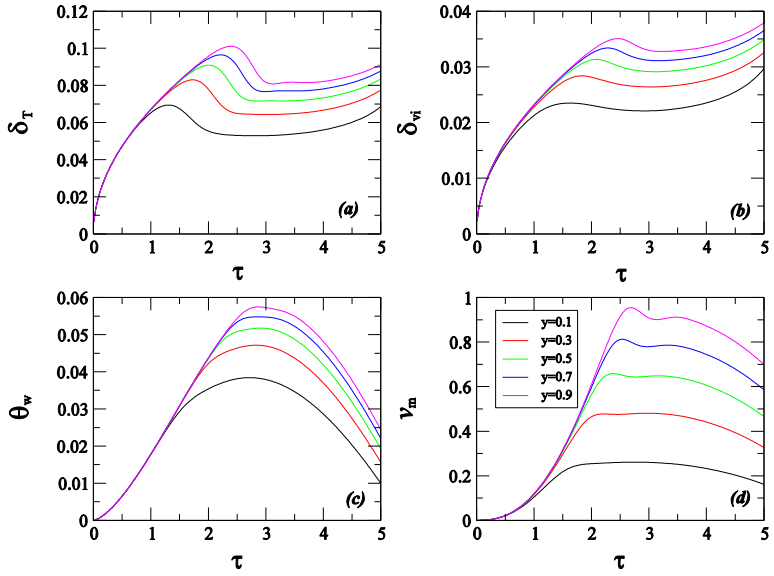

Figure 2. Time series of δ_T, δ_{vi}, θ_w, and v_m at y=0.1, 0.3, 0.5, 0.7 and 0.9 for the case of Ra=10^8, Pr=7 and f_n=0.1.

2. *At the dimensionless transition time scale τ_s:*

$$\delta_{T,s} \sim \left(\frac{2}{\pi}\right)^{1/5} \frac{\left(1+Pr^{-1/2}\right)^{2/5} y^{1/5}}{\left[\sin\left(2\pi f_n \tau_s\right)\right]^{1/5} Ra^{1/5}}, \tag{14}$$

$$\delta_{vi,s} \sim \left(\frac{2}{\pi}\right)^{1/5} \frac{y^{1/5}}{\left(1+Pr^{-1/2}\right)^{3/5}\left[\sin\left(2\pi f_n \tau_s\right)\right]^{1/5} Ra^{1/5}}, \tag{15}$$

$$\theta_{w,s} \sim \left(\frac{\pi}{2}\right)^{4/5} \frac{\left(1+Pr^{-1/2}\right)^{2/5}\left[\sin\left(2\pi f_n \tau_s\right)\right]^{4/5} y^{1/5}}{Ra^{1/5}}, \tag{16}$$

$$v_{m,s} \sim \left(\frac{\pi}{2}\right)^{2/5} \frac{\left[\sin\left(2\pi f_n \tau_s\right)\right]^{2/5} y^{3/5}}{\left(1+Pr^{-1/2}\right)^{4/5}}. \tag{17}$$

3. *At the quasi-steady state:*

$$\delta_{T,qs} \sim \left(\frac{2}{\pi}\right)^{1/5} \frac{\left(1+Pr^{-1/2}\right)^{2/5} y^{1/5}}{\left[\sin\left(2\pi f_n \tau\right)\right]^{1/5} Ra^{1/5}}, \tag{18}$$

$$\delta_{vi,qs} \sim \left(\frac{2}{\pi}\right)^{1/5} \frac{y^{1/5}}{\left(1+Pr^{-1/2}\right)^{3/5}\left[\sin\left(2\pi f_n \tau\right)\right]^{1/5} Ra^{1/5}}, \tag{19}$$

$$\theta_{w,qs} \sim \left(\frac{\pi}{2}\right)^{4/5} \frac{\left(1+Pr^{-1/2}\right)^{2/5}\left[\sin\left(2\pi f_n \tau\right)\right]^{4/5} y^{1/5}}{Ra^{1/5}}, \tag{20}$$

$$v_{m,qs} \sim \left(\frac{\pi}{2}\right)^{2/5} \frac{\left[\sin\left(2\pi f_n \tau\right)\right]^{2/5} y^{3/5}}{\left(1+Pr^{-1/2}\right)^{4/5}}. \tag{21}$$

Validation and quantification of scalings with numerical results

From the scalings, it is clear that the major parameters that govern the behavior of the unsteady natural convection boundary layer studied in this work are Ra, Pr, and f_n. To examine the effects of these three parameters on the scalings ten direct numerical simulation runs were performed; four

runs are at varying Ra (10^6, 10^7, 10^8, and 10^9, respectively) with fixed Pr=7 and f_n=0.1 for the Ra dependence; five runs are at varying Pr (3, 7, 20, 50, and 100, respectively) with fixed Ra=10^8 and f_n=0.1 for the Pr dependence; and three runs are at varying f_n (0.1, 0.025, and 0.01, respectively) with fixed Ra=10^8 and Pr=7 for the f_n dependence. All simulations were conducted in a dimensionless 2×2 computational domain with a mesh of 399×396 nodes. This mesh was chosen after a detailed mesh dependence test which ensures the simulation results obtained with it are mesh independent. The same code used in Lin and Armfield (1999, 2001, 2005, 2012) was used for these simulations. As the numerical methods, the construction and dependence test of the computational meshes, and the benchmarking of the code against the known theoretical results were well detailed in these references, these will not be repeated here.

1. *At the start-up stage*

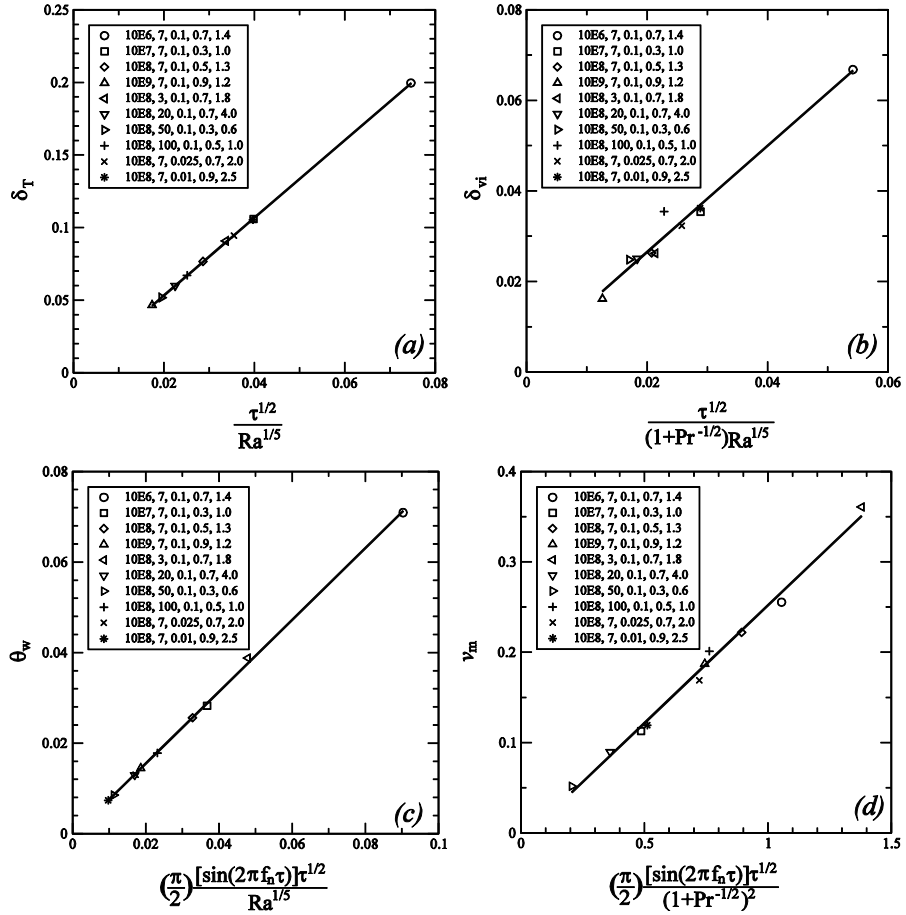

Figure 3. Validation and quantification of the scalings at the start-up stage with the numerical results.

The validation results for the scalings at the start-up stage are presented in Fig. 3, which clearly shows that all scalings are in good agreement with the numerical results as each scaling collapses the corresponding numerical results well onto a single straight line. The scalings are also quantified by the numerical results with a linear regression technique, giving the following quantified relations:

$$\delta_T = 2.676\frac{\tau^{1/2}}{Ra^{1/5}}, \tag{22}$$

$$\delta_{vi} = 1.251\frac{\tau^{1/2}}{\left(1+Pr^{-1/2}\right)Ra^{1/5}}, \tag{23}$$

$$\theta_w = 0.767\left(\frac{\pi}{2}\right)\frac{\sin(2\pi f_n \tau)\tau^{1/2}}{Ra^{1/5}}, \tag{24}$$

$$v_m = 0.261\left(\frac{\pi}{2}\right)\frac{\sin(2\pi f_n \tau)\tau^{3/2}}{\left(1+Pr^{-1/2}\right)^2}. \tag{25}$$

2. *At the dimensionless transition time scale* τ_s

The validation results for the scalings at the dimensionless transition time scale τ_s are presented in Fig. 4, which clearly shows that all scalings are also in good agreement with the numerical results as each scaling collapses the corresponding numerical results well onto a single straight line. The scalings are also quantified by the numerical results with the following quantified relations:

$$\delta_{T,s} = 3.906\left(\frac{2}{\pi}\right)^{1/5}\frac{\left(1+Pr^{-1/2}\right)^{2/5} y^{1/5}}{\left[\sin(2\pi f_n \tau_s)\right]^{1/5} Ra^{1/5}}, \tag{26}$$

$$\delta_{vi,s} = 1.775\left(\frac{2}{\pi}\right)^{1/5}\frac{y^{1/5}}{\left(1+Pr^{-1/2}\right)^{3/5}\left[\sin(2\pi f_n \tau_s)\right]^{1/5} Ra^{1/5}}, \tag{27}$$

$$\theta_{w,s} = 1.291\left(\frac{\pi}{2}\right)^{4/5}\frac{\left(1+Pr^{-1/2}\right)^{2/5}\left[\sin(2\pi f_n \tau_s)\right]^{4/5} y^{1/5}}{Ra^{1/5}}, \tag{28}$$

$$v_{m,s} = 1.053\left(\frac{\pi}{2}\right)^{2/5}\frac{\left[\sin(2\pi f_n \tau_s)\right]^{2/5} y^{3/5}}{\left(1+Pr^{-1/2}\right)^{4/5}}. \tag{29}$$

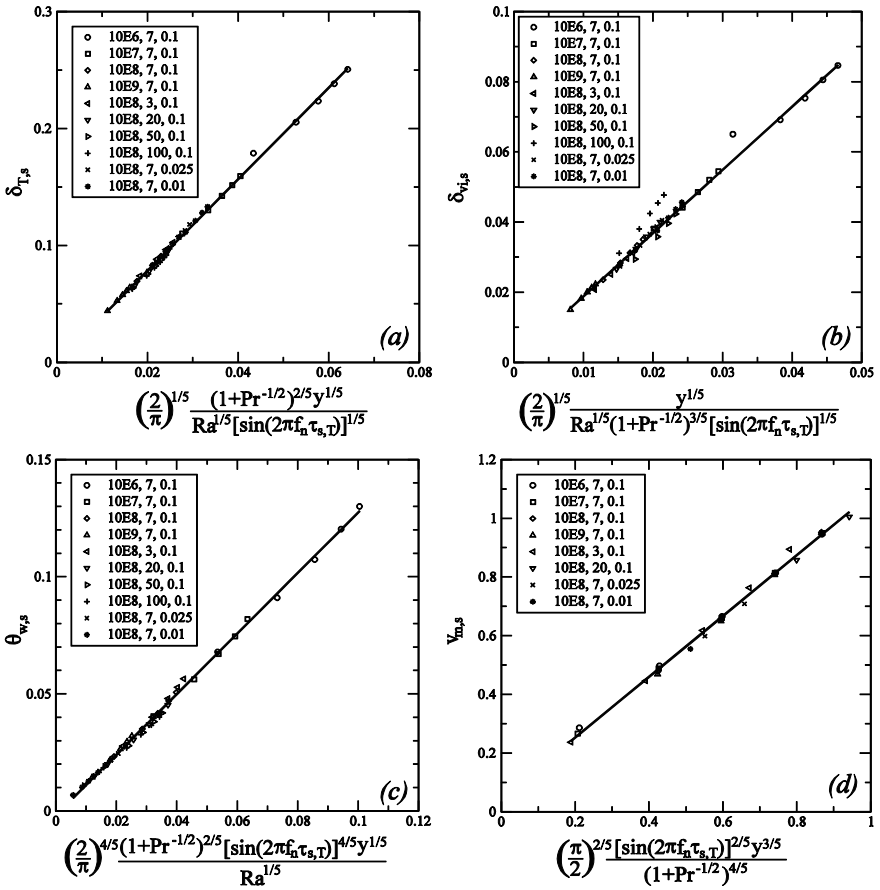

Figure 4. Validation and quantification of the scalings at the dimensionless transition time scale τ_s with the numerical results.

3. *At the quasi-steady state*

The validation results for the scalings at the quasi-steady state are presented in Fig. 5, which clearly shows that all scalings are again in good agreement with the numerical results as each scaling collapses the corresponding numerical results well onto a single straight line. The scalings are again quantified by the numerical results with the following quantified relations:

$$\delta_{T,qs} = 2.988\left(\frac{2}{\pi}\right)^{1/5} \frac{\left(1+Pr^{-1/2}\right)^{2/5} y^{1/5}}{\left[\sin\left(2\pi f_n \tau\right)\right]^{1/5} Ra^{1/5}}, \tag{30}$$

$$\delta_{vi,qs} = 1.640\left(\frac{2}{\pi}\right)^{1/5} \frac{y^{1/5}}{\left(1+Pr^{-1/2}\right)^{3/5}\left[\sin\left(2\pi f_n \tau\right)\right]^{1/5} Ra^{1/5}}, \tag{31}$$

$$\theta_{w,qs} = 1.684\left(\frac{\pi}{2}\right)^{4/5} \frac{\left(1+Pr^{-1/2}\right)^{2/5}\left[\sin\left(2\pi f_n \tau\right)\right]^{4/5} y^{1/5}}{Ra^{1/5}}, \tag{32}$$

$$v_{m,qs} = 0.1136 + 1.039\left(\frac{\pi}{2}\right)^{2/5} \frac{\left[\sin\left(2\pi f_n \tau\right)\right]^{2/5} y^{3/5}}{\left(1+Pr^{-1/2}\right)^{4/5}}. \tag{33}$$

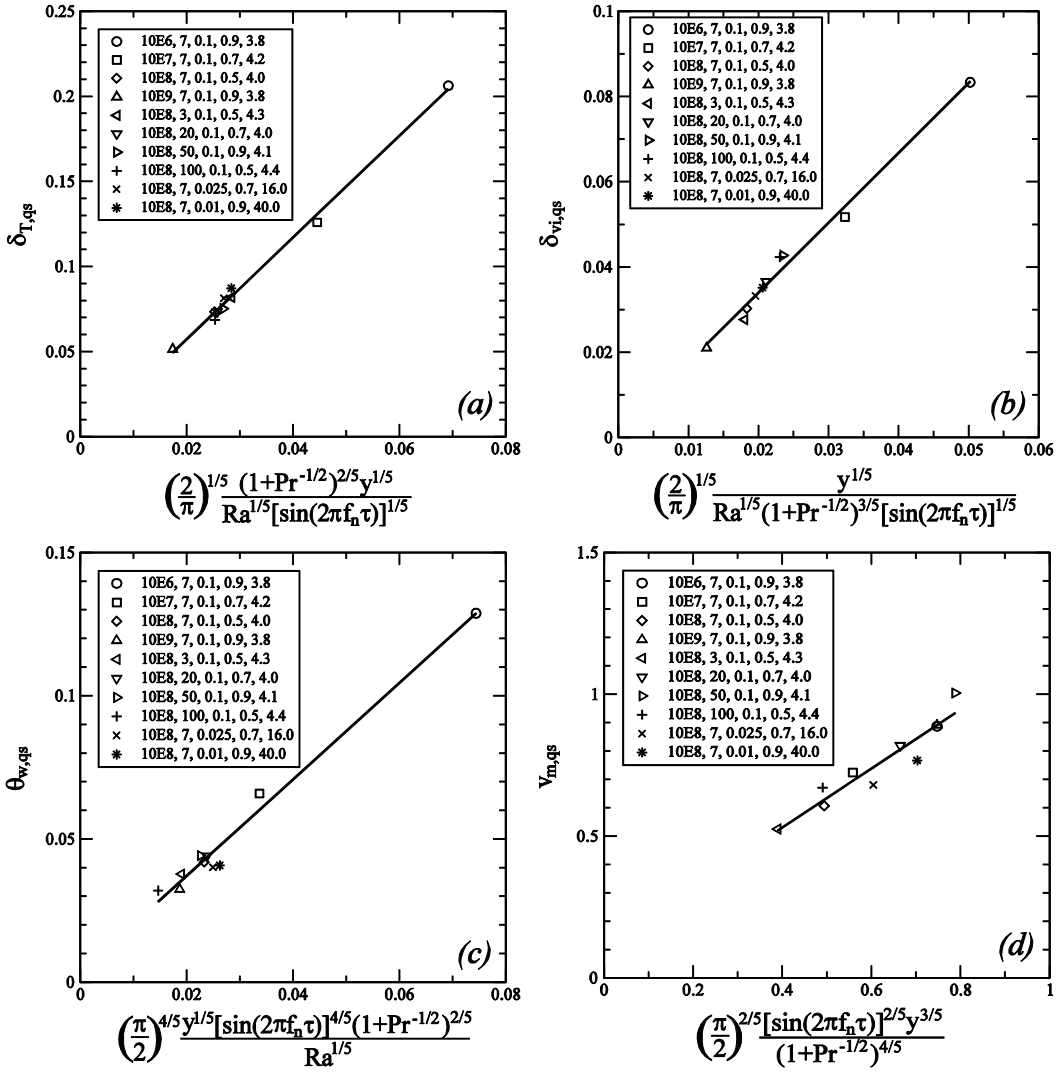

Figure 5. Validation and quantification of the scalings at the quasi-steady state with the numerical results.

Conclusions

In this paper, it was found that the transient and quasi-steady flow behavior of the unsteady natural convection boundary layer of a homogeneous Newtonian fluid with $Pr>1$ adjacent to a vertical plate evenly heated with a time-varying sinusoidal heat flux is controlled by the Rayleigh number, the Prandtl number, and the dimensionless natural frequency of the sinusoidal heat flux and is well represented by parameters such as the thermal boundary-layer thickness, the plate temperature, the viscous boundary-layer thickness, and the maximum vertical velocity within the boundary layer. The scalings developed for these parameters were compared with a series of direct numerical simulation, which clearly shows that these scalings in general predict the flow behavior very well, no matter at the start-up stage, or at the transition time scale which represents the end of the start-up stage and the beginning of the transitional stage of the boundary-layer development, or at the quasi-steady state.

Acknowledgments

The support from the National Natural Science Foundation of China (Grant No. 11072211), the Natural Science Foundation of Yunnan Province (2011FA017), the Program for Changjiang Scholars and Innovative Research Team in University of Ministry of Education of China, and the Australian Research Council is gratefully acknowledged.

References

Armfield, S. W., Patterson, J. C. and Lin, W. (2007), Scaling investigation of the natural convection boundary layer on an evenly heated plate. *Int. J. Heat Mass Transfer*, 50, pp. 1592–1602.

Bednarz, T. P., Lei, C. and Patterson, J. C. (2009), A numerical study of unsteady natural convection induced by iso-flux surface cooling in a reservoir model. *Int. J. Heat Mass Transfer*, 52, pp. 56–66.

Capobianchi, M. and Aziz, A. (2012), A scale analysis for natural convective flows over vertical surfaces. *Int. J. Thermal Sciences*, 54, 82–88.

Hyun, J. M. (1994), Unsteady buoyant convection in an enclosure. *Adv. Heat Transfer*, 24, pp. 277–320.

Lin, W. and Armfield, S. W. (1999), Direct simulation of natural convection cooling in a vertical circular cylinder. *Int. J. Heat Mass Transfer*, 42, pp. 4117–4130.

Lin, W. and Armfield, S. W. (2001), Natural convection cooling of rectangular and cylindrical containers. *Int. J. Heat Fluid Flow*, 22, pp. 72–81.

Lin, W. and Armfield, S. W. (2005), Scaling laws for unsteady natural convection cooling of fluid with Prandtl number less than one in a vertical cylinder. *Phys. Rev. E*, 72, article no. 016306.

Lin, W. and Armfield, S. W. (2012), Unified Prandtl number scaling for start-up and fully developed natural-convection boundary layers for both Pr>1 and Pr<1 fluids with isothermal heating. *Phys. Rev. E*, 86, article no. 066312.

Lin, W., Armfield, S. W. and Patterson, J. C. (2007), Cooling of a Pr<1 fluid in a rectangular container. *J. Fluid Mech*., 574, 85–108.

Lin, W., Armfield, S. W., Patterson, J. C. and Lei, C. (2009), Prandtl number scaling of unsteady natural convection boundary layers for Pr>1 fluids under isothermal heating. *Phys. Rev. E*, 79, article no. 066313.

Patterson, J. C. and Imberger, J. (1980), Unsteady natural convection in a rectangular cavity. *J. Fluid Mech*., 100, pp. 65–86.

Patterson, J. C., Lei, C., Armfield, S. W. and Lin, W. (2009), Scaling of unsteady natural convection boundary layers with a non-instantaneous initiation. *Int. J. Thermal Science*, 48, pp. 1843–1852.

Saha, S. C., Brown, R. J. and Gu, Y. T. (2012), Scaling for the Prandtl number of the natural convection boundary layer of an inclined flat plate under uniform surface heat flux. *Int. J. Heat Mass Transfer*, 55, 2394–2401.